IFSCC 2025 full paper (IFSCC2025-576)

Cutibacterium acnes-colonized Human Skin Equivalent Including Sebaceous Glands as a New Advanced 3D Model Mimicking Oily Skin and Acne-prone Skin for Active Ingredients Research

Julie RORTEAU[1], Sophie PECASTAINGS[2], *Esther MEDINA[3], Kilian LAHO[1], Cécile BIZE[2*]*, Julien LEBRAT[3], Marie-Océane CHAFFOIS[1], Amélie THEPOT[1], Aude ANTONIO[2], Pawel TULINSKI[3], Jérémy WELSCH[3], Morgan DOS SANTOS[1]

[1] LabSkin Creations, 69004 Lyon, France
[2] Seppic Research & Innovation, 81100 Castres, France
[3] Bioaster, 69007 Lyon, France

1. Introduction

Oily skin is a common dermatological condition characterized by excessive sebum production, enlarged pores, increased shininess, and a predisposition to blemishes and acne. While not a disease in itself, oily skin poses significant cosmetic concerns for consumers and contributes to the onset and the persistence of *acne vulgaris*, a multifactorial inflammatory disorder **[1]**. Acne development is closely linked to hyperactivity of sebaceous glands, follicular hyperkeratinization, inflammation, and the proliferation of *Cutibacterium acnes* (formerly *Propionibacterium acnes*), a lipophilic commensal bacterium that thrives in the sebum rich environment of the skin.

In the context of cosmetic science, the regulation of sebum production and the rebalancing of skin microbiota are key targets for developing innovative active ingredients aimed at improving the appearance and comfort of oily and acne-prone skin. However, the preclinical evaluation of such cosmetic ingredients has long been hindered by the lack of physiologically relevant *in vitro* models.

To date, most *in vitro* models used to study oily and acne-prone skin have been limited in complexity and physiological relevance. Conventional 2D cultures, often based on immortalized or stem cell–derived keratinocytes or sebocytes, provide limited insight into the multicellular and structural interactions occurring in human skin. While useful for high-throughput screening, these models lack the three-dimensional architecture, cellular diversity, and functional components, particularly sebaceous glands, necessary to accurately replicate acne pathophysiology **[2]**. More advanced 3D skin models have been developed, but they remain incomplete. The majority consist of reconstructed human epidermis (RHE), composed exclusively of keratinocytes, sometimes colonized with *C. acnes* to simulate acne-like inflammation **[3]**. Such models offer improved stratification but still lack sebaceous components and relevant gland/microbe interactions **[4]**. Over the past few years, some efforts have been made to introduce greater complexity. A skin organoid generated from pluripotent stem cells has been shown to include an epidermis, dermis, rudimentary pilosebaceous units, and neuronal elements **[5]**. While promising, this model is not optimized for *C. acnes* colonization or for evaluating active ingredients targeting oily skin. In another approach,

sebaceous glands have been cultured *ex vivo* following surgical extraction, but these models lack the surrounding epidermal and dermal context necessary for studying the full skin/microbiota interface **[6]**. To our knowledge, no existing model integrates functional sebaceous glands within a stratified epidermis while supporting colonization by *C. acnes*. This absence of a physiologically complete, reproducible, and microbiota-compatible *in vitro* model has remained a major obstacle to both mechanistic research and the development of innovative ingredients targeting oily and acne-prone skin.

To address this gap, we developed a full-thickness 3D human skin equivalent containing hiPSC-derived sebaceous glands and colonized with *C. acnes*, providing a new advanced *in vitro* platform to mimic oily and acne-prone skin for active ingredient research.

2. Materials and Methods

2.1 Ethical considerations and human cutaneous cell isolation

Human skin tissues were collected from surgical discards from anonymous healthy donors. Surgical residues were anonymized, and written informed consent was obtained from the patients in accordance with the ethical guidelines from Lyon University Hospital (Hospice Civils de Lyon) and approved by ethical committee of the Hospices Civils de Lyon according to the principles of the Declaration of Helsinki and Article L. 1243-4 of the French Public Health Code. All the samples used in this study belong to a collection of human skin samples declared to the French Research Ministry (Declaration no. DC-2024-6232 delivered to LabSkin Creations, Lyon, France). Primary cultures of human fibroblasts and keratinocytes were established from healthy skin biopsy obtained from an infant donor (<5 years old). iPSC-derived sebocytes were purchased from Phenocell (Grasse, France). Normal human epidermal keratinocytes (NHEKs) and dermal fibroblasts (NHDFs) were isolated from human skin.

2.2 Preparation of 3D reconstructed skin models

Briefly, 3D models were obtained by co-culturing NHDF and iPS-derived sebocytes on a scaffold composed of collagen, glycosaminoglycans, and chitosan (LabSkin matriX™, Lyon France) for 28 days. NHEK were subsequently seeded on top of the dermal equivalent and raised at the air/liquid interface to allow the epidermal formation **[2]**. 3D skin equivalent models (SEs), were cultured in optimized cell culture medium without antibiotics and antifungal. 3D skin equivalent models were treated with arachidonic acid (50 µM) added in the culture medium for 2 days to stimulate sebaceous gland formation. Arachidonic acid was depleted from the medium 24 h before *C. acnes* inoculation.

2.3 Bacterial strain cultivation, inoculation and quantification

C. acnes phylotype IA1 strains were commercially supplied (ATCC® 6919™ strain, ATCC, Manassas, VA, USA). *C. acnes* was grown in BHI in anaerobic conditions at 37 °C. To prepare suspensions, bacteria in the mid-exponential growth phase were suspended in PBS for 3D skin equivalent experiments. After 24 h arachidonic acid depletion, *C. acnes* was topically deposited either on epidermal side or on both dermal and epidermal sides of SEs. On day 49, SEs were inoculated with 50 µl of calibrated bacterial cultures at two doses 5.10^2 and 5.10^4 CFU/3D model for 2 hours. *C. acnes*-inoculated SEs were further co-cultured for 1, 3 and 7 days. At the end of the culture, bacterial counts in tissue biopsies (diameter = 4 mm) were determined by plating dilutions of homogenized biopsies in PBS + 0.1% Triton X-100. SE samples were also harvested for histological and immunohistological analysis and supernatants were collected for biochemical analysis. SEs were prepared in triplicate.

2.4 Histological analysis

Haematoxylin-phloxin-saffron staining

To evaluate the global cutaneous structure of samples, haematoxylin-phloxin-saffron (HPS) staining was performed. Paraffin sections of 5 µm of each condition were cut. After dewaxing and rehydration, the samples were stained with HPS. After rinsing, the sections were dehydrated before the mounting of the slides with a hydrophobic mounting medium.

Warthin Starry staining

Detection of bacteria within tissue sections was performed using the Warthin-Starry silver impregnation technique, optimized for bacteria staining. After deparaffinization and rehydration sections, slides were incubated in 1 % aqueous silver nitrate (Sigma-Aldrich, St. Louis, MO, USA) at 43–45 °C for 60 minutes in a dark humidified chamber. Following incubation, sections were rinsed twice in distilled water for 2 minutes each. A solution of 1 % silver nitrate and 0.1 % hydroquinone in 2 % aqueous gelatin was freshly prepared. Hydroquinone was prepared as a 0.1 % solution in warm 2 % gelatin. Slides were immersed in the developer at 43–45 °C and monitored closely for 1–2 minutes, until bacteria appeared black against a light-yellow background. Development was terminated by rinsing the slides thoroughly in distilled water. Sections were dehydrated through graded ethanol, cleared in xylene, and coverslipped using a synthetic resin mounting medium.

Nile Red staining

Nile Red and DAPI (4,6-diamidino-2-phenylindole) were used for the staining of neutral lipids and nuclei, respectively. Skin equivalent constructs were harvested and cryofixed with OCT compound. Labelling was performed on air-dried 5 µm cryosections and incubated for 30 minutes at RT in a solution containing 5 µg/mL of Nile Red and 1 µg/mL of DAPI in sterile PBS. Samples were washed twice with PBS before imaging under a fluorescence microscope.

2.5 Immunohistological analysis

For immunohistochemistry on paraffin sections, after heat-mediated antigen retrieval treatment, non-specific binding was blocked in PBS containing 4 % of BSA. Sections were then incubated with the primary antibodies against *C. acnes*, diluted at optimal concentration in PBS/BSA 4 %, overnight at room temperature. After incubation for 1 h with EnVision anti-mouse/rabbit-HRP secondary antibody (Dako EnVision$^+$, HRP) and apply DAB$^+$ substrate solution to the sections to reveal the colour of the antibody staining. Counterstain slides by immersing them in 25 % Harris Haematoxylin counterstaining solution.

For immunofluorescence, labeling was performed on air-dried 5 µm cryosections and incubated with primary antibodies against MUC-1. Secondary Alexa-568-conjugated anti-mouse (Molecular Probes, Invitrogen) were incubated 1h at room temperature. Nuclear counterstaining using DAPI was carried out routinely. As a negative control, the primary antibody was replaced by the corresponding IgG class.

2.6 Microscopic image acquisition and analysis

Immunostained specimens were observed using an Axio Observer A1/D1 optical microscope (Zeiss), and images were captured using AxioCam HRc (Zeiss) and ZEN 2 pro (Zeiss). Sixteen-bit images were saved in an uncompressed tagged image file format (tiff). Nine representative images were captured for each condition in the same manner.

For the markers of interest, positively red stained-tissue/cells areas were automatically detected and segmented from other pixels. Images were then converted in binary images, treated by mathematical morphology and sieved for isolating the regions of interest. The surface area of interest was measured automatically. Data were normalized by the total number of cells or the epidermal/dermal total surface area. Data are expressed in percentage of density.

2.7 Inflammation measurement: IL-1α and IL-8 Assays

IL-1α and IL-8 were measured by ELISA following manufacturer instructions (Raybiotech). All conditions were analyzed in triplicate, and the mean value and standard deviation were calculated for each condition. Results were expressed as a percentage effect relative to the untreated control.

2.8 Statistical analysis

For all data, the statistical significance was assessed running two-tailed Student's test, and statistically significant differences are indicated by asterisks as follows: *P < 0.05, **P < 0.01 and ***P < 0.001.

2. Results

Histological analysis of the sterile, full-thickness SE incorporating human induced pluripotent stem cell (hiPSC)-derived sebocytes revealed a highly organized and physiologically relevant tissue structure. Hematoxylin-Phloxine-Saffron (HPS) staining demonstrated a well-stratified epidermis overlaying a populated dermal compartment. Within this dermis, well-differentiated sebaceous gland-like structures were consistently observed. These 3D glandular organoids appeared embedded in a dense, eosinophilic neo-synthesized extracellular matrix (ECM), indicating active-matrix production by dermal fibroblasts.

As shown in Figure 1, the sterile SE model displayed various morphologies of sebaceous structures: isolated glandular units (View 1), closely adjacent or twin glandular formations (View 2), and, notably, branched glandular structures exhibiting clear duct-like extensions connecting to the basal layer of the epidermis (View 3). These duct-like structures are reminiscent of sebaceous ducts in native skin, which facilitate the delivery of sebum to the skin surface. Higher magnification of the boxed regions revealed lobular clusters of sebocyte-like cells with pale, lipid-rich cytoplasm and nuclear morphology consistent with sebocyte identity. The organized architecture and emergence of epidermis-connected ductal features underscore the functional maturation of the sebaceous organoids within the engineered tissue. The model maintained sterility throughout the culture period, allowing for controlled colonization by *Cutibacterium acnes* in subsequent experiments.

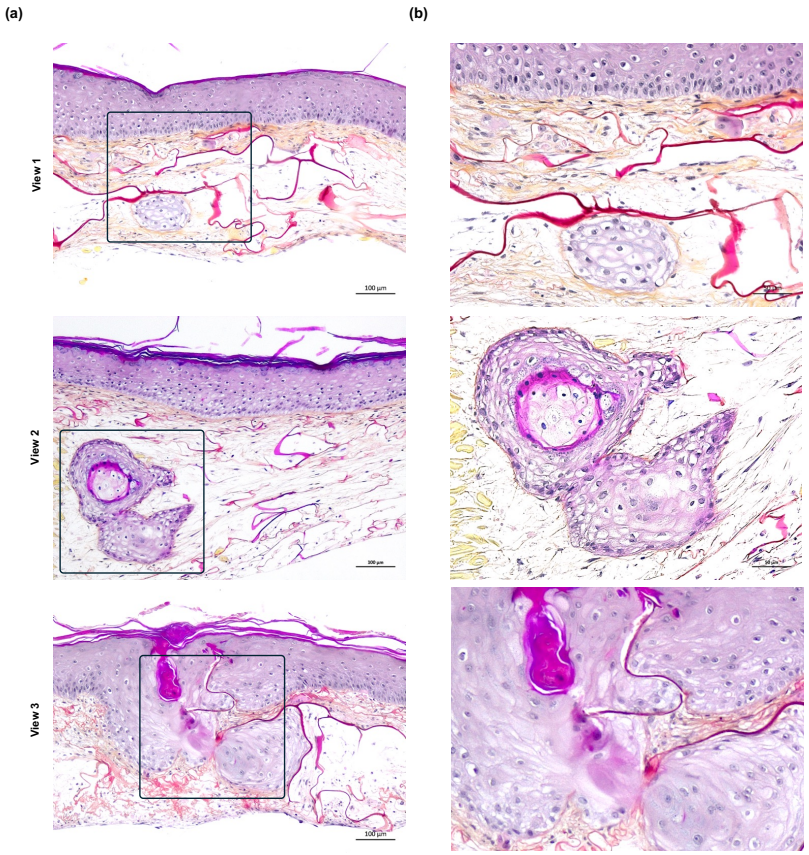

Figure 1. Histological analysis of sterile full-thickness human skin equivalents (SE) incorporating hiPSC-derived sebocytes.**(a)** Low-magnification HPS-stained sections of SEs from three independent views showing the overall tissue architecture, including a stratified epidermis and fibroblast-populated dermis. Boxed regions highlight sebaceous gland-like structures at different configurations: an isolated gland (upper panel, View 1), two closely positioned glands (middle panel, View 2), and a branched gland structure in direct contact with the basal epidermal layer (lower panel, View 3). Scale bar: 100µm.
(b) Higher magnification images of the boxed regions in (a) reveal well-organized sebaceous gland organoids composed of hiPSC-derived sebocyte-like cells. Scale bar: 50µm.

To further characterize the sebocyte-like cells within the glandular structures, tissue fluorescence analyses were performed (**Figure 2**). Nile Red staining revealed strong intracellular fluorescence within the organoids, indicating the presence of abundant neutral lipids and confirming active lipid synthesis typical of mature sebocytes (Figure 2a). In parallel, MUC-1 immunofluorescence showed clear expression in cells within the sebaceous structures, consistent with a sebocyte lineage (Figure 2b). These markers validated the sebaceous identity and functional differentiation of the hiPSC-derived sebocyte-like cells within the reconstructed SE.

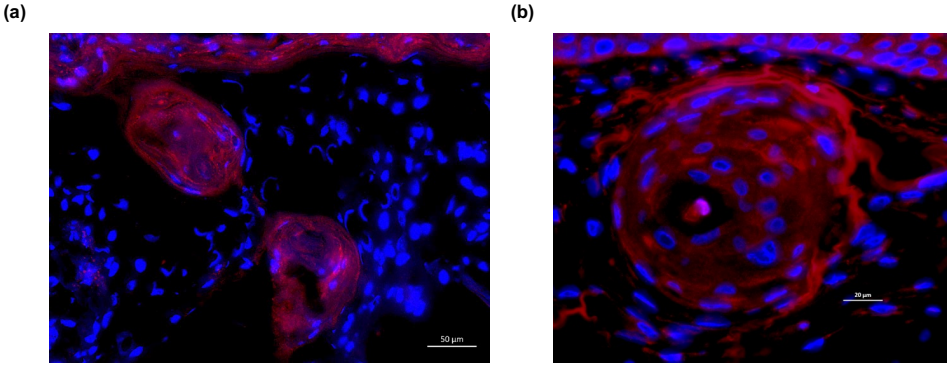

Figure 2. Fluorescence characterization of sebocyte-like cells in SE using Nile Red and MUC-1 staining. Fluorescence microscopy images of full-thickness SE sections containing hiPSC-derived sebocytes.
(a) Nile Red staining highlights intracellular neutral lipid accumulation (red) within sebocyte-like cells forming the sebaceous organoids, indicating active lipid production. Scale bar: 50 µm.
(b) MUC-1 immunostaining (red) confirms the expression of this sebocyte-associated marker within the glandular structures. Nuclei are counterstained with DAPI (blue). Scale bar: 20 µm.

3.2 C. acnes inoculation impacts significantly gland morphology and tissue architecture of 3D reconstructed SE including sebaceous glands

To promote bacterial growth in the 3D SE models including sebaceous glands, while maintaining physiological conditions representative of oily and acne-prone skin, several experimental parameters were tested: (i) bacterial inoculation method (epidermal-only *vs*. dual dermal/epidermal deposition); (ii) inoculum dose (5.10^2 CFU *vs*. 5.10^4 CFU), (iii) tissue-bacteria contact time (1 day *vs*. 7 days). The objective was to promote physiologically relevant colonization while preserving the structural and functional integrity of the sebaceous gland–containing 3D skin equivalent. Morphological analysis using HPS staining revealed that gland morphology and development, and tissue architecture were sensitive to inoculation parameters (Figure 3 a-b).

After 1 day, the condition combining epidermal-only deposition of 5.10^2 CFU preserved tissue organization, with a multilayered epidermis and well-defined sebaceous gland structures (Figure 3a - arrows). In contrast, high-dose inoculation (5.10^4 CFU) and/or dual-side application led to progressive tissue degradation and gland disorganization, particularly after 7 days (Figure 3b - arrows). Histological analysis of epidermal thickness showed at 5.10^2 CFU condition a significant reduction in both epidermal and dual-side colonization conditions, compared with the sterile control (Figure 3c). A significant increase in the number of glands / sections was observed in colonized tissues. More specifically, small glands (small (S) < 100 µm; medium (M) 100 to 200 µm; large (L) 200 to 300 µm; extra-large (XL) > 300 µm) were in greater number in 3D the models exposed to *C. acnes* (Figure 3c). The number of very large glands were increased when *C. acnes* was inoculated at 5.10^4 CFU/tissues on both skin sides.

These glands could result from the fusion of several glands. Under all conditions, the glands were functional and able to secrete lipids, with sebocytes expressing MUC-1 (data not shown).

After 7 days, the sterile 3D models were still well stratified, but the number of glands was significantly reduced. The presence of *C. acnes* significantly altered the structure of the tissues, independently of the mode of inoculation: the glands were rare and generally atrophied. The epidermis was much thinner and the tissues were strongly damaged. Purple patches, probably bacterial clumps, were visible beneath the dermis.

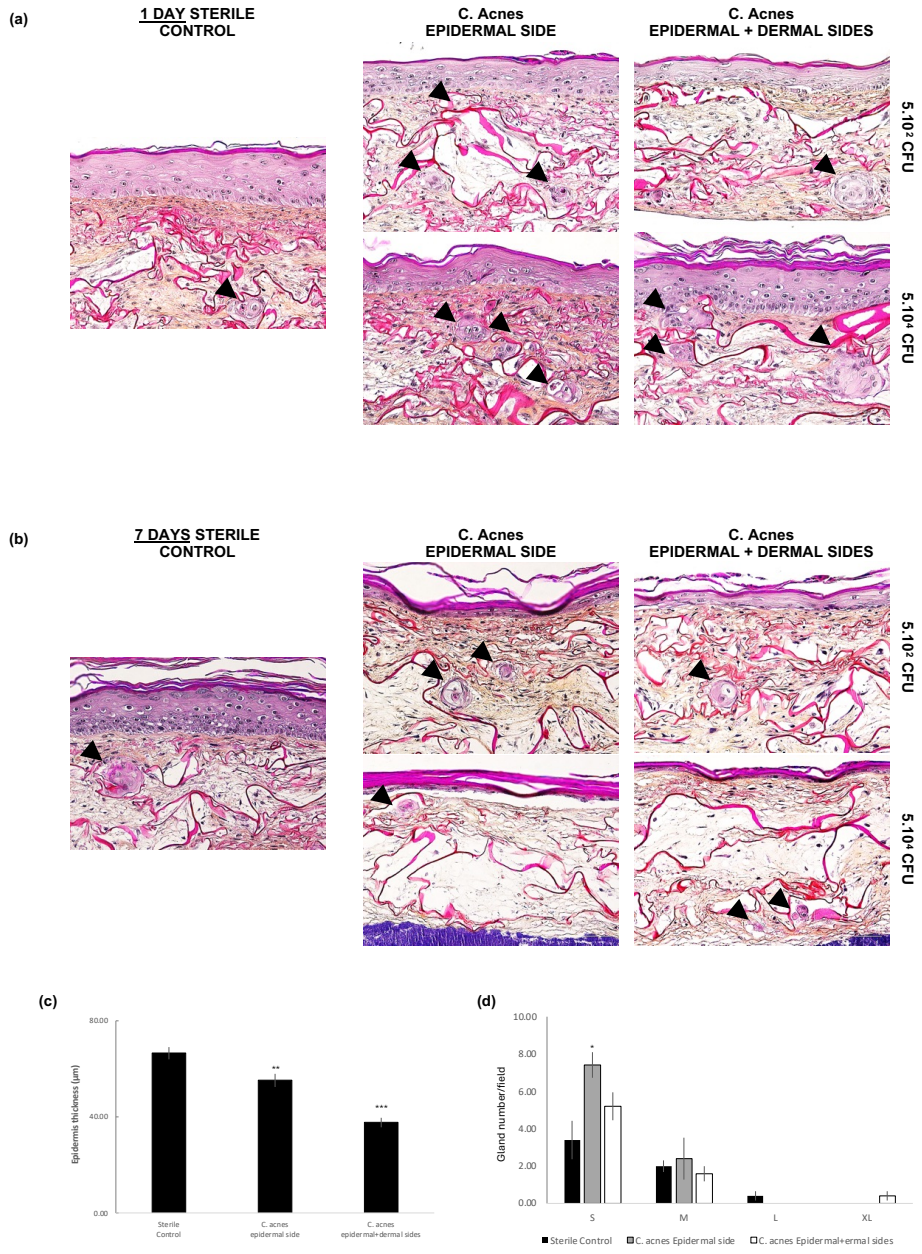

Figure 3. Structural impact of *C. acnes* colonization on the 3D sebaceous skin equivalent under varying conditions. **(a, b)** HPS-stained cross-sections after 1 day (a) and 7 days (b) of *C. acnes* colonization *via* epidermal-only or dual dermal/epidermal inoculation at 5.10² or 5.10⁴ CFU. Arrowheads indicate sebaceous gland structures. **(c)** Quantification of epidermal thickness after 1 day of exposure at 5.10² CFU. **(d)** Gland size and number classification under the same conditions at 5.10². S: small; M: medium; L: large; XL: extra-large.

To verify that the bacteria were maintained and/or proliferated in the tissues over time, punch biopsy samples were collected and bacteria were quantified on agar plates (Figure 4). After 1 day, *C. acnes* was not quantifiable (detected in only 38 % of the replicates). Seven days post-inoculation, the bacterial concentration increased significantly and reached approximately 10^6 CFU/punch. Neither the inoculation method nor the initial load had a significant impact on the bacterial colonization of tissues after 1 day or 7 days.

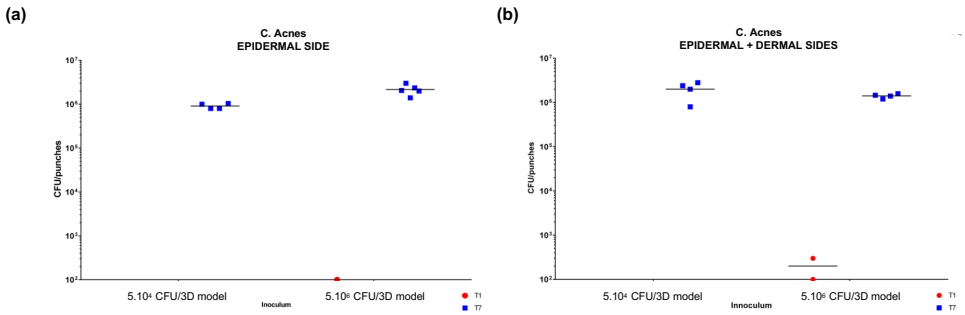

Figure 4. (a) Quantity of bacteria/punch biopsies in 3D tissues, inoculated on the epidermal side only, at 1 day (in red) and at 7 days (in blue). **(b)** Quantity of bacteria per sample in 3D model inoculated on the both epidermal and dermal sides, at 1 day (in red) and at 7 days (in blue).

Overall, none of the tested inoculation conditions proved fully optimal, as they either compromised tissue integrity or failed to sustain balanced colonization, highlighting the need for further refinement to promote *C. acnes* growth in sebaceous gland–containing 3D skin models while preserving physiological features representative of oily and acne-prone skin.

3.5 Three days C. acnes colonisation promotes bacterial growth in the 3D skin models including sebaceous glands, while maintaining physiological conditions representative of oily and acne-prone skin

Following the limitations observed with shorter exposures and extreme bacterial doses, we refined the experimental protocol to better support *C. acnes* colonization under physiologically relevant conditions. An intermediate inoculum of 5.10^3 CFU was selected and applied simultaneously to both the epidermal and dermal sides of the 3D sebaceous skin equivalent. The models were then cultured for 3 days to allow sustained bacterial interaction while preserving tissue viability and sebaceous gland structure.

Histological analysis confirmed the effectiveness of this approach. As shown in Figure 4a, HPS staining revealed preserved epidermal stratification and well-defined sebaceous gland–like structures in the colonized models (right panel), comparable to the sterile control (left panel). Warthin-Starry staining further demonstrated the presence of *C. acnes* in the upper dermis and in close proximity to sebaceous glands, confirming successful and spatially relevant colonization.

To validate bacterial presence and localization, immunohistochemical detection was performed using a polyclonal anti-*C. acnes* antibody (PAB). As shown in Figure 4b, brown immunostaining was clearly detected near and inside sebaceous structures in colonized tissues. Deconvolution of the same image enhanced the visualization of the bacterial signal, confirming *C. acnes* localization around and inside glandular regions and validating the Warthin-Starry findings.

Confocal microscopy with Nile Red (Figure 4c) further supported the preservation, and even enhancement of sebocyte functionality under the optimized colonization conditions. Low-

magnification views (upper panels) revealed a well-organized tissue architecture in both sterile and *C. acnes*–colonized SE, with clearly visible lipid-rich sebaceous gland–like structures. Notably, high-magnification images (lower panels) showed that sebaceous structures in the colonized condition appeared larger and exhibited more intense Nile Red staining compared to the sterile control. These observations indicate that *C. acnes* exposure not only preserved sebocyte morphology but also stimulated intracellular lipid accumulation. This suggests an activating effect of *C. acnes* on sebocyte secretory function, consistent with its known role in modulating the lipid-rich microenvironment of acne-prone skin. At 3 days, 4.4 ± 0.3 log CFU/punch (viable and culturable bacteria) were detected (data not shown).

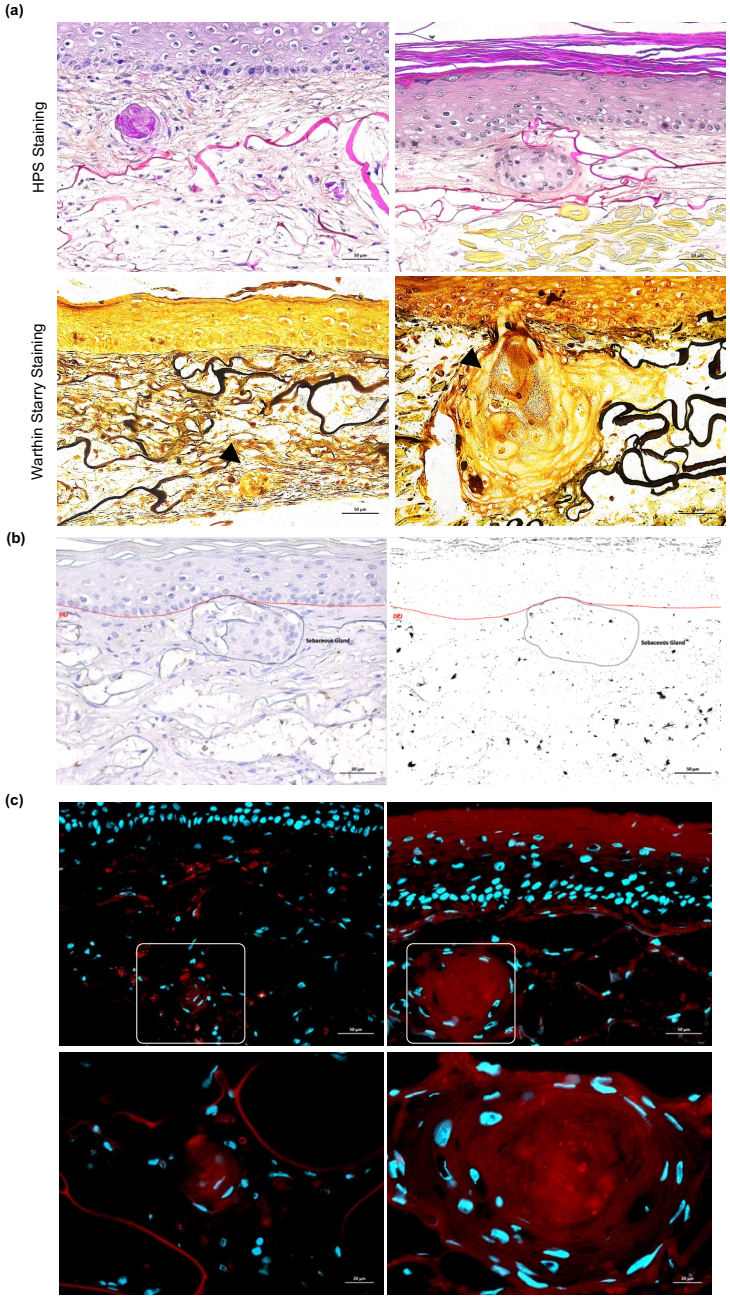

Figure 5. Histological and confocal imaging of 3D Sebaceous skin models colonized by *C. acnes* for 3 days under optimized conditions. **(a)** Representative HPS (top row) and Warthin-Starry (bottom row) stainings of 3D sebaceous SE after 3 days under either sterile conditions (left) or *C. acnes* colonization (right; 5.10^3 CFU, dual epidermal and dermal deposition). Glands are indicated by arrows. **(b)** Immunohistochemical detection of *C. acnes* using a polyclonal anti-C. acnes antibody (PAB). Left:

Representative brightfield image showing positive bacterial signal (brown). Right: Digital deconvolution of the same image enhances signal detection and contrast. **(c)** Confocal microscopy of Nile Red (red; neutral lipids) and DAPI (blue; nuclei) staining under sterile (left) and *C. acnes* colonized (right) conditions. Upper panels: low-magnification views show overall tissue organization and lipid-rich sebaceous structures. Lower panels: high-magnification images. Scale bars = 50 µm (low magnification), 20 µm (high magnification).

3.6 C. acnes triggers a time-dependent inflammatory response in the 3D sebaceous skin model

To evaluate the inflammatory response induced by *C. acnes*, levels of IL-8 and IL-1α were measured in sterile and colonized 3D sebaceous skin models at 1 day and 3 days (Figure 6). At 1 day, IL-8 levels showed no significant change between conditions (+13%), while IL-1α levels increased moderately (+32%) in the colonized model. By 3 days, both cytokines were significantly elevated: IL-8 by 49% and IL-1α by 42% compared to controls. These results demonstrate that *C. acnes* induces a progressive inflammatory response over time, mimicking early features of acne-prone skin while maintaining tissue integrity.

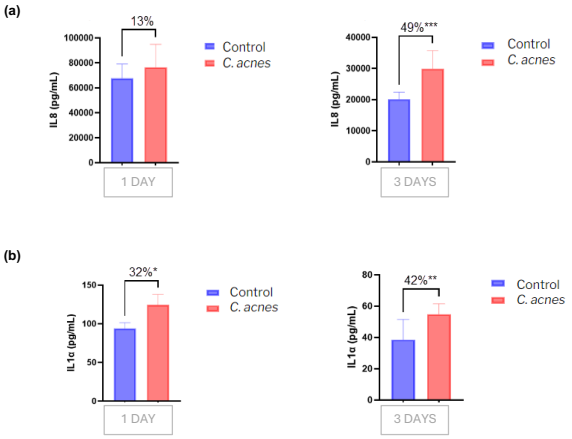

Figure 6. Inflammatory cytokine secretion in sterile and Cutibacterium acnes–colonized 3D sebaceous skin models. Quantification of pro-inflammatory cytokines IL-8 (a) and IL-1α (b) in culture supernatants of sterile controls (blue) and C. acnes–colonized models (red) after 1 day and 3 days of exposure (5 × 10^3 CFU, dual deposition). Data are expressed as mean ± SEM.

4. Discussion

The primary objective of this study was to develop and validate a novel 3D *in vitro* skin model that mimics key features of acne-prone skin, including functional sebaceous glands and colonization by *C. acnes*. The data demonstrate the successful establishment of such a model, highlighting its structural and biological relevance for studying host–microbe interactions in oily skin.

A major advance of this model lies in the incorporation of hiPSC-derived sebocytes capable of organizing into functional sebaceous gland-like structures within a stratified epidermis and ECM-rich dermis. This glandular formation within the tissue context reflects a level of complexity not achieved in conventional 2D sebocyte cultures or in 3D models lacking dermal or sebaceous components. It underscores the importance of a supportive 3D microenvironment to enable sebocyte organization and functional lipid production.

The presence of *C. acnes* was shown to modulate the morphology and distribution of sebaceous structures. After 3 days of colonization, the number of glands increased significantly, with a shift toward smaller gland size. These findings suggest that *C. acnes* may influence sebaceous gland dynamics, potentially by affecting sebocyte turnover or sebum

metabolism-processes known to play a role in acne pathophysiology. This observation aligns with the *in vivo* association of *C. acnes* with lipid-rich, sebaceous environments and early gland remodeling in acne lesions.

The model also recapitulates the early inflammatory events typical of acne-prone skin. While IL-1α and IL-8 levels decreased over time in sterile models, likely reflecting reduced stimulation following initial tissue differentiation, a significant increase in both cytokines was observed in *C. acnes*–colonized tissues after 3 days. This confirms the capacity of *C. acnes* to induce a measurable inflammatory response and supports its role in initiating or sustaining inflammation in acne [7, 8]. Importantly, this activation occurred without structural degradation of the tissue, indicating that the model maintains a physiological balance between host defense and tissue integrity. The production and release of various pro-inflammatory cytokines and chemokines by skin cells, induced by C. acnes is well known. This occurs through the activation of Toll-like receptors (TLR2 [9] and TLR4 [10]) upon recognition of *C. acnes's* pathogen-associated molecular patterns (PAMPs). The activation of these receptors leads to downstream signaling pathways like NF-κB and MAPK, which ultimately result in the expression of genes encoding inflammatory mediators. To the best of our knowledge, this is the first *in vitro* skin model that combines full-thickness architecture with functional sebaceous glands and supports standardized *C. acnes* colonization. Previous models have typically been limited to keratinocyte-only RHEs, isolated sebaceous structures, or complex organoids that are not compatible with microbial exposure. This model fills a critical gap by enabling the study of gland/microbe/epidermis interactions in a controlled, reproducible, and physiologically relevant context. This platform offers new opportunities for mechanistic studies and ingredient screening. It can be used to evaluate active compounds targeting sebum regulation, microbial balance, or inflammation under conditions that closely reflect human acne-prone skin. Future developments may include integration of immune cells or hair follicle components to further enhance the model's relevance for studying acne pathogenesis and testing therapeutic strategies.

5. Conclusion

This study presents a novel and physiologically relevant 3D in vitro skin model that successfully mimics key features of oily and acne-prone skin. By incorporating functional sebaceous glands derived from hiPSCs and supporting controlled *Cutibacterium acnes* colonization, the model captures both the structural and biological complexity required to study early acne mechanisms. The optimized colonization protocol using a moderate inoculum, dual epidermal and dermal deposition, and a 3-day exposure enabled sustained bacterial growth while preserving epidermal integrity, sebaceous gland morphology, and lipid production. Importantly, this setup induced a measurable inflammatory response consistent with early-stage acne, without compromising tissue structure. Together, these findings demonstrate that this 3D sebaceous skin model offers a powerful tool for investigating *C. acnes*/host interactions and evaluating active ingredients targeting sebum regulation, microbiota balance, and inflammation. It provides a robust, reproducible platform for advancing preclinical research and developing new strategies for treating oily and acne-prone skin.

References

[1] Dreno B, et al. J Eur Acad Dermatol Venereol. 2015;29(Suppl 4):1–14.
[2] Kligman AM, et al. Arch Dermatol. 1976;112(2):263–8.
[3] Laclaverie M, et al. Skin Pharmacol Physiol. 2021;34(6):360–9.
[4] Vitroscreen. Technical documentation.
[5] Lee J, et al. Nature. 2020;582(7812):399–404.
[6] De Bengy C, et al. Exp Dermatol. 2019;28(7):799–803.
[7] Hong JY, et al. Front Med (Lausanne). 2025 Jan 29;12:1518382
[8] Sim JK, et al. Pharmaceuticals (Basel). 2025 Jan 9;18(1):71
[9] Mayslich C, et al. Int J Mol Sci. 2022 May 3;23(9):5065
[10] Noh HH, et al. PLoS One. 2022 Aug 10;17(8):e0268595.